

Capping and Passivation of Aluminum Nanoparticles: Aluminum-Induced Alkene Polymerization

B. Thomas^{*}, E. Lloyd^{*}, E. Guliants,^{**} C. Bunker,^{***} P. Jelliss^{*}, and S. Buckner^{*}

^{*}Saint Louis University, St. Louis, MO, USA, buckners@slu.edu, jellissp@slu.edu

^{**}University of Dayton Research Institute, Dayton, OH, USA

^{***}Air Force Research Laboratory, Propulsion Directorate, Wright-Patterson Air Force Base, OH, USA

ABSTRACT

We report here on the use of alkenes as passivating agents for aluminum nanoparticles (Al NPs). These core-shell materials have high active Al contents (>70%) and increased air stability (~15 weeks). The electron-rich Al core appears to initiate alkene polymerization, as is shown by the absence of alkene resonances in FTIR spectra. We also present results from PXRD, DSC, and TGA which support the presence of metallic Al along with TEM images which yield particle size and morphology information.

Keywords: aluminum nanoparticles, alkenes, polymer shells

1 INTRODUCTION

In the presence of H₂O and O₂, aluminum nanoparticles (Al NPs) readily react to form Al₂O₃ and H₂(g). The H₂(g) by-product can be utilized for alternative fuel and high-density energy storage applications.^[1] In addition, metallic Al NPs have been shown to improve the combustion rates and energy output of liquid fuels.^[2] However, Al's extreme instability in the presence of H₂O is problematic with respect to synthesis and long-term storage. To overcome this hurdle, a capping agent is introduced which passivates the exposed Al NP surface while serving as a prophylactic barrier towards premature oxidation and hydrolysis. Ideally, the capping agent should aid in the formation of monodisperse Al NPs with high elemental Al contents. Polymer coatings are one potential option for achieving effective Al NP capping. The polymer shell thickness can be modified to provide maximum protection to the Al core by varying factors such as reaction time and degree of polymerization

We have previously reported on the use of alkyl-substituted epoxides as passivating agents for Al NPs.^[3,4] The electron-rich Al core serves as a polymerization initiator, leading to the formation of a monolayer of polyether loops on the nascent Al NP surface. Epoxydodecane, epoxyhexane, and epoxyisobutane were explored as capping agents. The effects of varying the epoxide's alkyl chain length were explored, with epoxydodecane yielding Al NPs with the highest degree of air stability. Use of epoxyisobutane as the passivating agent resulted in pyrophoric materials.

More recent work has focused on the synthesis of Al NPs capped with 1,2-epoxy-9-decene.^[5] This alkene-terminated epoxide cap yields nanoparticles displaying minimal reactivity towards H₂O and high active Al contents that can be maintained in an ambient atmosphere for ~6 weeks. By thermal activation, polymerization of the epoxide's terminal alkene functionality is induced, leading to the envelopment of the Al NPs in a hydrophobic polymer matrix. We found that by incorporating a cross-linking agent into the polymer matrix (1,13-tetradecadiene), Al NPs displaying extreme long-term air stability (~80% active Al content after 1 year air exposure time) could be produced.

Here we report on the use of alkenes as capping agents for Al NPs. This work is significant as the electron-rich Al surface appears to initiate alkene polymerization in the absence of a free-radical initiator. Powder X-ray diffraction (PXRD), differential scanning calorimetry (DSC), and thermogravimetric analysis (TGA) results are presented to confirm the presence of metallic Al while Fourier-transform infrared spectroscopy (FT-IR) is used to analyze the organic capping layer. Through Al speciation and titrimetric analysis, unprecedentedly high active and total Al contents of ~90% and ~60%, respectively, were determined. In addition, we found these materials to be extremely air-stable, maintaining high active Al contents for ~15 weeks. This is extremely significant considering only ~40% of the samples were comprised of the organic capping material.

2 EXPERIMENTAL

2.1 Reagents and Materials

N,N-Dimethylethylamine alane (0.5M in toluene), titanium (IV) isopropoxide [Ti(O_iPr)₄, 99.999% trace metals basis], 1,7-octadiene (98%), 1,9-decadiene (98%), 1,13-tetradecadiene (90%), 1-octene (98%), 1-decene (94%), 1H, 1H, 2H – perfluoro – 1 – decene (99%), toluene (anhydrous, 99.8%), ethylenediaminetetraacetic acid disodium salt dihydrate, zinc sulfate heptahydrate (99.999% trace metal basis), sodium acetate trihydrate (≥98.0%), sodium hydroxide (≥98.0%), and nitric acid (70%) were all supplied by Sigma-Aldrich. Sodium chloride was provided by Fisher Scientific. Both AlH₃ and Ti(O_iPr)₄ were stored under argon atmosphere to prevent O₂ exposure. All capping agents were subjected to several freeze-pump-thaw cycles to remove any dissolved oxygen. Toluene was

distilled over sodium metal under argon atmosphere to remove water.

2.2 Synthesis

All materials were synthesized following the AlH_3 decomposition method initially reported by Buhro with a few modifications.^[6,7] First, a clean, dry round-bottom flask, purged 3 times with argon, was charged with AlH_3 (6.5 mL, 0.00325 mol) and toluene (15 mL). The resulting clear solution was heated to 85°C with vigorous stirring. Once the desired temperature was reached, 0.8 mL $\text{Ti}(\text{O}_i\text{Pr})_4$ (0.8 mL, 0.0334M in toluene) was added followed by the immediate addition of a stoichiometric amount of the capping agent (see Table 1). Upon addition of $\text{Ti}(\text{O}_i\text{Pr})_4$, an immediate color change from clear to brown was observed along with $\text{H}_2(\text{g})$ evolution. This mixture was vigorously stirred and refluxed at 85°C for 30 minutes. All solvent was then removed, and the resulting gray solid was heated *in vacuo* at 85°C overnight.

2.3 Active & Total Al Content Determination

Speciation of Al was determined using a modification of a previously reported method in which ~50 mg of the synthesized Al NPs were reacted with concentrated NaOH in a glass retort.^[8] The glass retort was attached to a buret filled with saturated NaCl(aq) to prevent H_2 dissolution. By monitoring the NaCl level within the buret, the amount of evolved $\text{H}_2(\text{g})$ was determined. Through use of stoichiometry and the Ideal Gas Law, the amount of active, unoxidized Al present in the sample was determined.

The total Al content was determined via a compleximetric Zn^{2+} -EDTA back titration.^[9] First, concentrated HNO_3 was added to the Al(III)/ NaOH mixture until a color change of yellow to clear was observed. The resulting mixture was then diluted into either a 250.00 mL or 500.00 mL volumetric flask, and 25.00 mL of this Al solution were added to 10.00 mL of a 0.1000M secondary standard EDTA solution. The pH of the aluminum/ EDTA solution was then adjusted to 7, followed by the addition of 10 mL sodium acetate buffer solution (pH=5). This Al/ EDTA/ buffer solution was then boiled for ~5 minutes to ensure complete complexation of the Al to the EDTA. Following heating, the solution was back-titrated with a 0.05000M primary standard ZnSO_4 solution with the use of xylenol orange (yellow to pink color change) as the indicator.

2.4 CHARACTERIZATION

All powder X-ray diffraction (PXRD) experiments were performed on a Rigaku Ultima IV diffractometer equipped with a Cu source operated at 40kV and a scintillation counter detector. The presence of face-centered cubic (fcc) Al was confirmed by comparison with

the appropriate pattern from the ICDD Crystallographic Database. The presence of elemental Al was also determined using a TA Instruments model Q2000 DSC (differential scanning calorimeter) and a TA Instruments model Q500 TGA (thermogravimetric analyzer). Samples were analyzed from 25°C - 725°C using a 10°C/min temperature profile. A Shimadzu model FTIR-8400S spectrometer equipped with an attenuated total reflectance (ATR) attachment was used to analyze the organic capping layer. All TEM images were captured using a FEI Inspect F50 SEM (scanning electron microscope) equipped with a STEM detector. Samples were cast on Formvar grids provided by Ted Pella.

3 RESULTS AND DISCUSSION

Table 1 lists all the different alkenes tested as capping agents for our Al NPs. Dark gray powders with high active Al contents were produced (Table 1). As mentioned in the procedural notes, a variety of Al: cap molar ratios were tested, with the 10:1 Al: cap molar ratio yielding materials with the highest active Al contents. Determination of the active Al content of Al NPs capped with the perfluoro-alkene proved difficult as a result of the formation of a yellow foam-like substance upon reaction with NaOH; however, H_2 production did eventually occur upon reaction with H_2O accompanied with sonication.

All materials were analyzed using electron microscopy, and the results are shown in Figure 1. The particles are spherical and appear to be ~30 nm in diameter; however, particle aggregates are present which lead to difficulty in size analysis. Sonication can be used to break up the aggregates; however, some inter- and intranoparticle cross-linkage occurs as a result of interactions between the terminal alkene groups of the dienes. Electron micrographs for the Al NPs capped with the monoalkenes are currently not available for comparison, however.

Capping Agents	Structure	Active Al Contents
1-octene		90%
1-decene		89% ± 3%
1H, 1H, 2H – perfluoro – 1 – decene		80% ± 3%
1,7-octadiene		83% ± 6%
1,9-decadiene		80% ± 6%
1,13-tetradecadiene		78% ± 5%

Table 1. List of alkenes used as capping agents for Al NPs along with active Al contents (0 day air exposure).

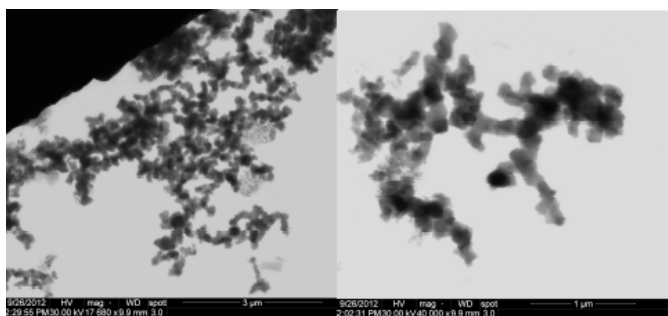


Figure 1. STEM images of Al NPs capped with decadiene (10:1 Al: cap molar ratio).

Aging studies were conducted to determine the decomposition rate of these materials. Previous work has shown that an oxide layer, 2-6 nm thick, forms immediately on the Al NP surface upon air exposure, with complete oxidation of the Al NP core occurring several days following air exposure.^[10] The aging behavior for the diene-capped Al NPs has been explored, and a representative plot of active Al content as a function of air exposure time is shown in Figure 1. Zero order decay is observed, with the active Al content decreasing linearly from 90% to 55% over a 15 week ambient air exposure period. Aging studies for the simple alkene-capped Al NPs are still in progress. We believe that the oxidation of the monoalkene-capped Al NPs will occur at a faster rate than the oxidation of the diene-capped Al NPs. Inter- and intra- nanoparticle cross-linking is not expected for the monoalkene-capped particles as only one reactive functional group is present in these monomers.

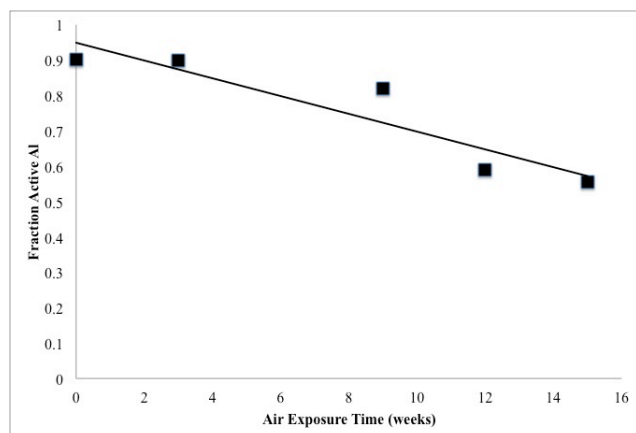


Figure 2. Plot showing active Al content of octadiene-capped Al NPs as a function of air exposure time.

A representative PXRD pattern for the alkene-capped Al NPs is shown in Figure 3. The peaks centered at $2\theta \approx 39^\circ, 45^\circ, 65^\circ, 79^\circ,$ and 83° correspond to the (100), (200), (220), (331), and (222) lattice planes, respectively, reported for face-centered cubic (fcc) Al. No evidence of Al_2O_3 is observed; however, this is not unexpected as the oxide layer is normally amorphous. Utilizing the Scherrer Equation, Al

core sizes of ~ 25 nm were estimated, thus correlating with the Al core sizes seen from TEM.

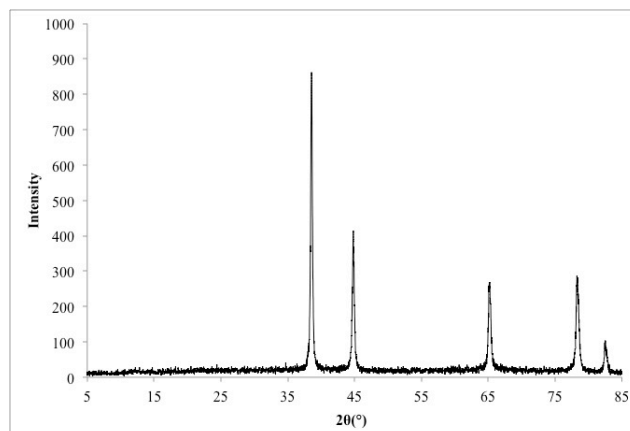


Figure 3. PXRD pattern for Al NPs capped with octadiene (10:1 Al: cap molar ratios).

Figures 4 and 5 show the DSC and TGA results for the various diene-capped Al NPs (10:1 Al: cap molar ratios). At 560°C , exotherms are observed in the DSC that can be attributed to the $\text{Al} \rightarrow \text{Al}_2\text{O}_3$ transition. The aforementioned transition is accompanied by a large mass increase observed at 560°C in the TGA. The large mass increases are indicative of samples with very high total Al contents. The initial mass losses seen between $\sim 200\text{C}-450^\circ\text{C}$ result from the combustion of the hydrocarbon capping layer.

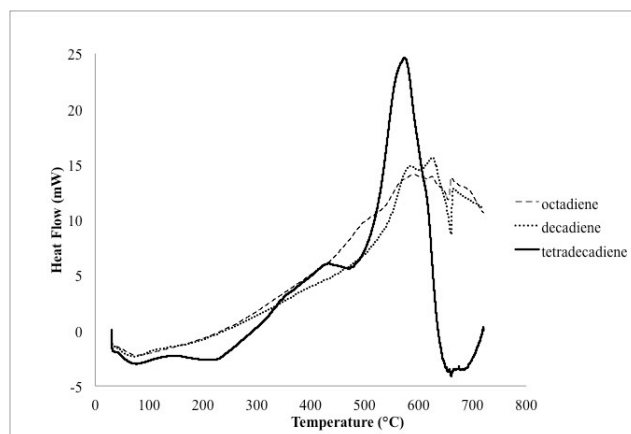


Figure 4. DSC results for Al NPs capped with octadiene, decadiene, and tetradecadiene (10:1 Al: cap molar ratios).

Interesting variations are observed in the DSC curves for the diene-capped Al NPs. The Al ignition event is much more distinct for tetradecadiene-capped Al NPs than for both octadiene-capped Al NPs and decadiene-capped Al NPs. The longer alkyl chain length of tetradecadiene creates a higher degree of steric hindrance at the Al core/ cap interface. As a result, interactions between the individual diene monomers are limited, leading to a more monodisperse capping layer. A higher degree of

polydispersity within the organic passivating shell results in polymer combustion events occurring over a much broader temperature range. This process potentially hinders the nano-Al ignition process, causing incomplete combustion. The presence of Al metal melting endotherms corresponding at 660°C in the DSC curves for both octadiene- and decadiene-capped Al NPs lends credence to this theory.

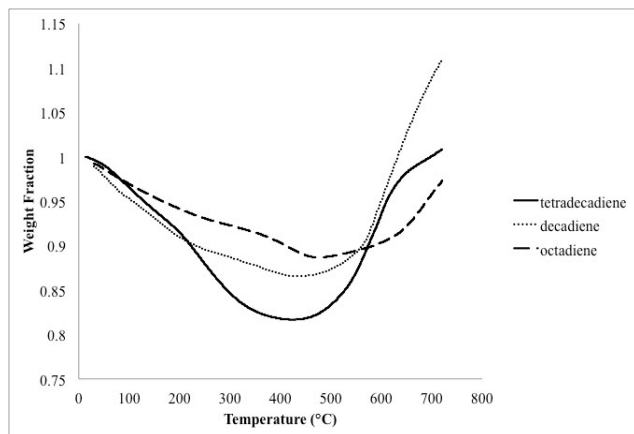


Figure 5. TGA results for Al NPs capped with octadiene, decadiene, and tetradecadiene (10:1 Al: cap molar ratio).

The nature of the organic passivating layer is probed via attenuated total reflectance Fourier-transform infrared spectroscopy (ATR-FTIR) (Figure 4). The passivating layer is composed solely of carbon and hydrogen atoms; therefore we expect to see C-H stretching modes, which are definitely present in the 2850-2950 cm^{-1} region. Most notably, there are no peaks associated with C=C, which would be present at 1650 cm^{-1} . This is indicative of alkene activation by the electron-rich Al core.

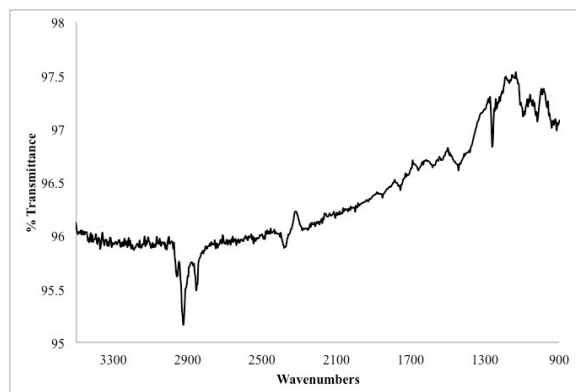


Figure 6. ATR-FTIR of Al NPs capped with tetradecadiene (10:1 Al: cap molar ratio).

4 CONCLUSIONS

We have utilized catalytic AlH_3 decomposition for the synthesis of air-stable Al NPs capped by a variety of dienes. These materials display minimal reactivity in water along with high active Al contents. In terms of active Al content,

octadiene was determined to be the best capping agent for these materials; however, DSC/TGA experiments lend support towards tetradecadiene being the most effective alkene capping agent. Active Al contents of 50% are observed for octadiene-capped Al NPs following a 15-week air exposure period, a significant discovery as these materials are composed mainly of Al/Al^{3+} . Most notably, FT-IR confirms the polymerization of alkenes on the nascent Al NP surface in the absence of a polymerization initiator. Further experiments are underway to fully characterize the nature of this interaction. In addition, further work needs to be completed on monoalkene-capped Al NPs to allow for further comparison with diene-capped Al NPs. In addition, the effects of using a perfluorinated alkene as an Al NP capping agent will be explored, with particular emphasis on the effects of fluorine atoms towards alkene reactivity.

5 ACKNOWLEDGEMENTS

We thank the US Air Force Nanoenergetics Program for funding. Acknowledgement is made to the National Science Foundation for support under grant CHE-0963363 for renovations to the research laboratories in Monsanto Hall.

REFERENCES

- [1] C. E. Bunker, M. J. Smith, K. A. S. Fernando, B. A. Harruff, W. K. Lewis, J. R. Gord, E. A. Guliants, D. K. Phelps, *ACS Appl. Mater. Inter.*, 2, 11–14, 2010.
- [2] H. Tyagi, P. E. Phelan, R. Prasher, R. Peck, T. Lee, J. R. Pacheco, P. Arentzen, *Nano Lett.*, 8, 1410–1416, 2008.
- [3] S. W. Chung, E. A. Guliants, C. E. Bunker, D. W. Hammerstroem, Y. Deng, M. A. Burgers, P. A. Jelliss, S. W. Buckner, *Langmuir*, 25, 8883–8887, 2009.
- [4] D. W. Hammerstroem, M. A. Burgers, S. W. Chung, E. A. Guliants, C. E. Bunker, K. M. Wentz, S. E. Hayes, S. W. Buckner, P. A. Jelliss, *Inorg. Chem.*, 50, 5054–5059, 2011.
- [5] B. J. Thomas, C. E. Bunker, E. A. Guliants, S. E. Hayes, A. Kheyfets, K. M. Wentz, S. W. Buckner, P. A. Jelliss, *J. Nanopart. Res.*, in press, 2013.
- [6] J. A. Haber, W. E. Buhro, *J. Am. Chem. Soc.*, 120, 10847–10855, 1998.
- [7] K. T. Higa, C. E. Johnson, R. A. Hollins, *US Pat.* 5885321, 1999.
- [8] O. G. Glotov, V. Zyryanov, *Arch. Combust.*, 11, 251–262, 1991.
- [9] S. P. Yang, R. Y. Tsai, *J. Chem. Ed.*, 83, 906, 2006.
- [10] C. E. Aumann, G. L. Skofronick, J. A. Martin, *J. Vac. Sci. Technol. B*, 13, 1178–1183, 1995.